A novel approach to crystallisation of nanodispersible microparticles by spray drying for improved tableting

*Krzysztof J. Paluch, Lidia Tajber, Bozena Adamczyk, Owen I. Corrigan, Anne Marie Healy**

School of Pharmacy and Pharmaceutical Sciences, Trinity College Dublin, College Green, Dublin 2, Ireland.

* To whom correspondence should be sent. Tel.: +353-1-896-1444, Fax: +353-1-896-2810, e-mail: healyam@tcd.ie

Abstract

High-dose API powders which are to be tableted by direct compression should have high compactibility and compressibility. This note reports on a novel approach to the manufacture of crystalline powders intended for direct compaction with improved compactibility and compressibility properties. The poorly compactable API, chlorothiazide, was spray dried from a water/acetone solvent mix producing additive-free nanocrystalline microparticles (NCMPs) of median particle size 3.5 μm. Tablets compacted from NCMPs had tensile strengths ranging from 0.5 to 4.6 MPa (compared to 0.6-0.9 MPa for tablets of micronised CTZ) at compression forces ranging from 6 kN to 13 kN. NCMP tablets also had high porosities (34-20%) and large specific surface areas (4.4 to 4.8 m^2/g). The time taken for tablets made of NCMPs to erode was not statistically longer ($p>0.05$) than for tablets made of micronised CTZ. Fragmentation of NCMPs on compression was observed. The volume fraction of particles below 1 μm present in the suspension recovered after erosion of NCMP tablets was 34.8±3.43%, while no nanosized particles were detected in the slurry after erosion of compacted micronised CTZ.

Keywords: spray drying, tabletability, specific surface area, nanocrystalline microparticles, erosion, nanosuspension

Graphical abstract

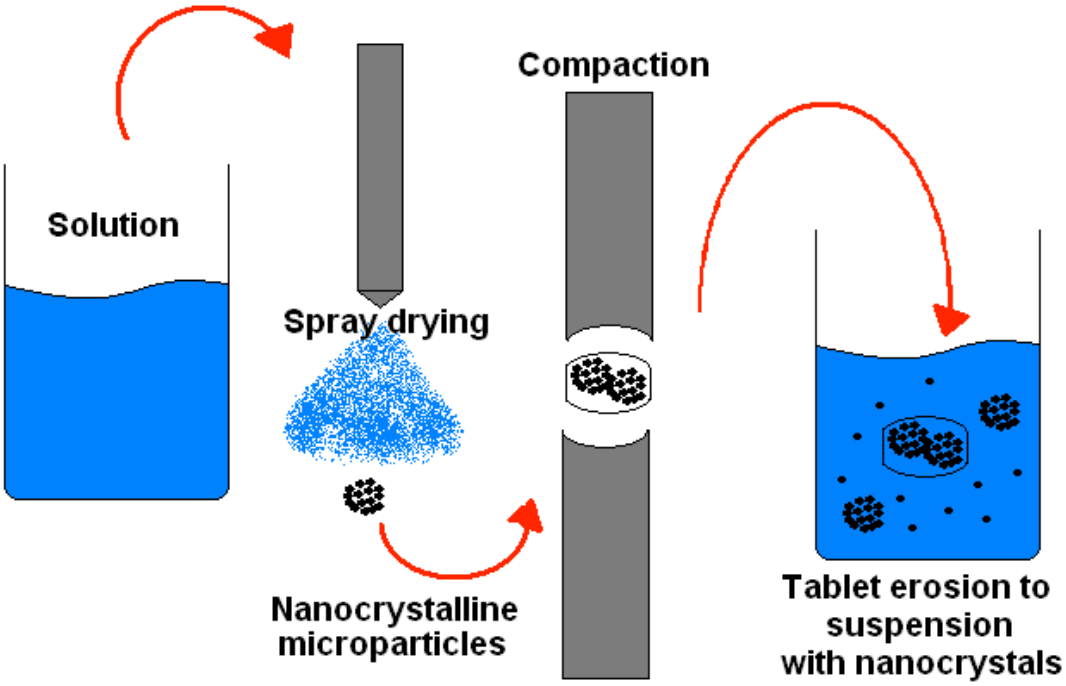

The issues of tabletability of an API are important when the tablet is composed predominantly of the API (Augsburger and Hoag, 2008). Spray drying (SD) has been shown to improve tabletability of direct compression fillers such as lactose (SDL). Although SDL is an effective binder only at high loads over >80%, it is consequently not suitable in formulations of containing high-dose, poorly compactible APIs (Augsburger and Hoag, 2008).

In the field of pharmaceutical nanotechnology, SD has been used to isolation of nanoparticles (Vergote et al., 2001) or to produce amorphous nanoparticles (Chow and Sun, 2004). Dolenc et al. (2009) reported on tableting of SD celecoxib nanoparticles, however assessed tablets comprised blends with microcrystalline cellulose. Limitations associated with production of nanoparticles include particle size control during precipitation/crystallisation, separation/drying of nanoparticles, conversion in a dry form and finally redispersion from powder to nanosuspension. Preparation of microparticles comprising nanocrystals can thus be regarded as a convenient approach to alleviate some of these limitations. Healy et al. (2008) reported that SD from a mixture of solvents can result in the formation of amorphous nanoporous microparticles, but no reports on nanocrystalline microparticles (NCMPs) manufactured using the mixed solvent approach have been published to date.

This work presents SD/crystallisation of NCMPs composed of chlorothiazide (CTZ), a high-dose API, previously shown to be crystalline when SD (Corrigan et al., 1984). The tabletability and erosion characteristics of NCMPs is assessed and compared to conventionally processed powders.

SD of CTZ (Sigma, Germany) samples using conditions as outlined in table 1 was performed using a Büchi B-290 Mini Spray Dryer (Büchi 93001 en). Tablets (n=10) were compressed using a MTCM 1 tablet press (GlobePharma, USA), supplied with concave 10 mm diameter tooling. Tablets (n=10) were subjected to hardness test using Dr. Schleuniger-6D tablet tester (Pharmatron, UK). Erosion studies were performed in a vertically held glass vial (7.5x2 cm), equipped on the bottom with a 2 mm wire mesh and a tubing pumping in and out erosion medium (15 ml of 0.1M HCl at 37 ˚C) at the flow rate of 30 ml/min. Erosion time was defined as the time when all tablet fragments have passed through the wire mesh. Obtained suspensions were introduced to wet laser diffraction particle size analysis performed in 0.1 M HCl using a Hydro μP attachment with no ultrasound, using the pump speed of 1000 rpm and initial obscuration of 20±2%. Solubility studies of CTZ in solvents were carried out in a shaking water bath at 50 rpm, for 24 hours in 25 ˚C. Excess of CTZ was loaded into 10 ml glass vials, suspended in 5 ml of the solvent and vials hermetically sealed. The suspensions were filtered through a 0.2 μm membrane filter. Quantities of dissolved CTZ were assessed using UV spectrophotometry as described before (Paluch et al., 2010). Differential scanning calorimetry (DSC), thermogravimetric analysis (TGA), powder XRD (PXRD) analysis, Fourier transform infrared spectroscopy (FTIR), scanning electron microscopy (SEM), specific surface area analysis (T_{BET}) and particle size analysis by laser diffraction (dry method) were performed as described before (Paluch et al., 2011 and Tajber et al., 2009).

The solubilities of CTZ in pure water (W) and acetone (AC) were 0.02% and 0.88% w/v, respectively. A maximum solubility of CTZ of 5.4% (w/v) in AC/W mixes was determined at 0.9 AC volume fraction (Fig. A1.). The 9:1 AC/W v/v solvent mix was therefore selected for SD as the higher the SD feed concentration the greater may be the yield of the recovered powder. The

concentration of CTZ in the liquid was set initially to 5% w/v (CTZ5). The recovered particles were spherical and smooth (Fig. 1). The T_{BET} of the sample was measured to be ~2.3 m^2/g (Table 1).

As CTZ5 did not render nanocrystallites, the feed concentration was decreased 10-fold (CTZ0.5). The CTZ0.5 particles were spherical with rough, porous surfaces (Fig. 1). CTZ0.5 presented an increased $T_{BET,}$ ~10-fold comparing with CTZ starting material powder (CTZRaw) and 2-fold in comparison to CTZ5 (Table 1). Particle size analysis showed that feed concentration had a significant ($p<0.05$) effect on the median particle size (d(50)) of SD CTZ. The d(50)s were 4.7 (CTZ5) and 2.6 μm (CTZ0.5) (Table 1).

SD from 0.5% CTZ w/v solution resulted however in a low production yield of about 51% and it was deemed unsatisfactory for tablet production. Therefore another batch of CTZ was produced using a feed concentration of 2% w/v (CTZ2). The change in feed concentration resulted in the production of microparticles composed of prismoidal nanocrystallites (Fig.1), with only a slight reduction of process yield to ~89% in comparison to CTZ5. SD of CTZ2 was carried out in the open blowing mode (in nitrogen atmosphere), mimicking the setup of industrial spray dryers. The T_{BET} of CTZ2 was measured to be ~4 m^2/g with the d(50) of 3.5 μm.

All CTZ SD samples were PXRD crystalline. The peak patterns were consistent with CTZRaw (Fig. A2). The DSC traces of CTZ5, CTZ0.5 and CTZ2 were superimposable with CTZRaw, with melting points ranging from ~370 °C to ~360 °C (~363.5 ˚C for CTZRaw, Fig. A3). TGA analysis indicated the residual solvent content for all SD systems was in the range from 0.1 to 0.2%. FTIR presented no visible band changes occurring in CTZ pre- and past-processing and all spectra of the samples were superimposable (Fig. A4).

CTZRaw, CTZ5, CTZ2 as well as Dipac™, a commonly used direct compression binder/filler, were subjected to tableting. Compaction of CTZ5 in the range from 3 to 13 kN compression force (F) resulted in the production of either very brittle and fragile or

capped/laminated tablets thus only CTZ2 was investigated further. Tablets made of Dipac^{TM} at F as low as 3 kN presented a force to tensile failure (P) of 23.7±6.6 N (Fig. 2). The P values increased linearly with F at the rate of 23.6 N/kN (Table A1). In comparison, for CTZRaw the P values initially increased with increasing F and then fell off at F over 10 kN. The P values comparable to Dipac^{TM} compressed at 3 kN was recorded for CTZRaw only at F at and above 6 kN (Fig. 2). CTZ2 presented improved compactibility of the API. The tablet formed at 3 kN had a P value of 26.5±23.85 N, which was slightly higher than for Dipac^{TM}, but the rate of change of P versus F of 8.1 N/kN was nearly 3 times lower than for Dipac^{TM}.

Among Dipac^{TM}, CTZRaw and CTZ2 the largest porosity, of 33.74%, was recorded for the CTZ2 system at F of 3 kN (Fig.3). Tablets formed from CTZRaw at 6 kN had lower porosity of 20.5% and significantly ($p<0.05$) lower tensile strength (σ_t) of 0.6 MPa in comparison to those formed from CTZ2 (Fig. 2). Also the porosity of CTZRaw was higher than for Dipac^{TM} at 6 kN F and Dipac^{TM} presented a greater σ_t of 1.08 MPa. The porosity of CTZ2 tablets decreased by about 13.5% while σ_t increased by 4.1 MPa.

Analysis of changes of T_{BET} of Dipac^{TM} (Fig. 4) indicated that the original T_{BET} of 0.2 m^2/g measured for powder started to increase when compacted at 3 and 6 kN. The T_{BET} reached a plateau at 10 kN. In contrast to Dipac^{TM}, CTZRaw did not show a tendency of T_{BET} to decrease over the range of tested compression forces from 6 to 13 kN. The T_{BET} measured for the powder (0.51 m^2/g) was seen to increase in tablets. This indicated that CTZRaw compacted into tablets predominantly due to crushing and interlocking. CTZ2 behaved differently. The T_{BET} of loose powder was 3.92 m^2/g and increased slightly for the material compressed under 3 kN to 4.75 m^2/g and under 6 kN to 4.8 m^2/g, only to drop to 4.44 m^2/g when F of 10 kN was applied.

Tablets with comparable tensile strength, CTZRaw compressed at 6 kN and CTZ2 compressed at 3 kN, were subjected to erosion studies. Tablets made of CTZRaw eroded in 13±4 min, while CTZ2 tablets eroded in 17±3 min. No significant differences ($p<0.05$) in the 10th

percentile diameter (d(0.1)), d(0.5) and fractions of particles below 0.2 μm (<0.2 μm) and 1 μm (<1 μm) were observed for uncompressed particles of CTZRaw and suspension of eroded CTZRaw tablets (Table 2). This suggests that compaction of CTZRaw does not affect the micromeritic properties of the particles.

In contrast, d(0.1), d(0.5) and fractions <0.2 μm and <1 μm were all statistically different for uncompressed CTZ2 and suspension of eroded CTZ2 tablets (Table 2). The d(0.1) and d(0.5) values were lower for the sample collected from erosion studies compared with the equivalent values for the uncompressed CTZ2, while the <0.2 μm and <1 μm fractions were significantly ($p<0.05$) greater (5.7±0.3% versus 27.3±4.6% and 18.1±1.9% versus 34.8±3.4%, respectively) for the eroded tablet and uncompressed CTZ2, respectively. This is consistent with the observation depicted in Fig. 4 showing that T_{BET} increased upon compaction of CTZ2 at 3kN suggesting that fragmentation of NCMPs occurs when tableted.

In conclusion, NCMPs of CTZ presented improved tabletability, as observed from the force to tensile failure, tensile strength and tablet porosity versus compression force relationships, in comparison to micronised and SD nonporous CTZ. The NCMPs also maintained large T_{BET} on compression. Up to approximately 35% (by volume) of nanoparticulate material were observed to be released from the compacted NCMPs. The approach presented here whereby nanoparticles may be crystallised, dried and agglomerated to form microparticles in a one-step continuous process by SD presents a simplification over other production processes for nanocrystals/nanoparticles.

Acknowledgements

The authors wish to acknowledge funding for this research from Solid State Pharmaceutical Cluster (SSPC), supported by Science Foundation Ireland under grant number 07/SRC/B1158.

References

Augsburger, L.L., Hoag, S.W., 2008. Pharmaceutical dosage forms: Tablets, Third edition, Vol. 2 Rational design and formulation, Informa Healthcare USA Inc.

Büchi 93001 en Operation manual Mini Spray Dryer B-290

Chow, L.C., Sun, L., 2004. Properties of Nanostructured Hydroxyapatite Prepared by a Spray Drying Technique. J. Res. Natl. Inst. Stand. Technol. 109, 543-551.

Corrigan, O.I., Holohan, E.M., Sabra, K., 1984. Amorphous forms of diuretics prepared by spray drying. Int. J. Pharm., 18, 195–200.

Dolenc, A., Kristl, J., Baumgartner, S., Planinšek O., 2009. Advantages of celecoxib nanosuspension formulation and transformation into tablets. Int. J. Pharm. 376, 204–212.

Healy, A.M., McDonald, B.F., Tajber, L., Corrigan, O.I., 2008. Characterisation of excipient-free nanoporous microparticles (NPMPs) of bendroflumethiazide. Eur. J. Pharm. Biopharm., 69(3), 1182-6.

Kristmundsdottir, T., Gudmundsson, O.S., Ingvarsdottir, K., 1996. Release of diltiazem from Eudragit microparticles prepared by spray-drying. Int. J. Pharm., 137, 159-165.

Paluch, K.J., Tajber, L., McCabe, T., O'Brien, J.E., Corrigan, O.I., Healy, A.M., 2010. Preparation and solid state characterisation of chlorothiazide sodium intermolecular self assembly suprastructure, Eur. J. Pharm. Sci., 41, 603–611

Paluch, K.J., Tajber, L., McCabe, T., O'Brien, J.E., Corrigan, O.I., Healy, A.M., 2011. Preparation and physicochemical analysis of crystalline forms of chlorothiazide potassium Eur. J. Pharm. Sci., 42, 220–229.

Vergote, G.J., Vervaet, C., Van Driessche, I., Hoste, S., De Smedt, S., Demeester, J., Jain, R.A., Ruddy, S., Remon, J.P, 2001. An oral controlled release matrix pellet formulation containing nanocrystalline ketoprofen. Int. J. Pharm. 219, 81–87.

Tajber, L., Corrigan, D.O., Corrigan, O.I., Healy, A.M., 2009. Spray drying of budesonide, formoterol fumarate and their composites—I. Physicochemical characterisation. Int. J. Pharm. 367, 1–2, 79-85.

Tables

Table 1. List of the analysed samples, with SD conditions, production yields, specific surface areas (T_{BET}) and median particle size (d(50)) for the various CTZ samples and Dipac™.

Sample	**Solvent system**	**Feed conc. [% w/v]**	**Inlet temp [°C]**	**Outlet temp [°C]**	**Yield [%]**	**Mode***	**T_{BET} [m^2/g]**	**d(50) [µm]**
CTZraw	N/A	N/A	N/A	N/A	N/A	N/A	0.50±0.00	12.6±0.1
CTZ5	AC/W 9:1 v/v	5.0	80	54	~95	CM	2.26±0.06	4.7±0.1
CTZ0.5	AC/W 9:1 v/v	0.5	80	53	~51	CM	4.55±0.07	2.6±0.1
CTZ2	AC/W 9:1 v/v	2.0	120	99	~89	OM	3.9±0.13	3.5±0.1
Dipac™	N/A	N/A	N/A	N/A	N/A	N/A	0.21±0.03	178.4±0.6

* AC-acetone, W-water, OM–open mode, CM-closed mode. Regardless on the drying mode the feed rate was set to 10 ml/min and drying gas flow rate of 473 norm litres per hour was used.

Table 2. Particle size distribution characteristics (d(0.1) and d(0.5)) and fraction of particles below 0.2 and 1 µm in 0.1M HCl for sample CTZRaw and CTZ2 before compression (P CTZRaw) and (P CTZ2) and suspensions recovered after erosion (T CTZRaw) and (T CTZ2) (n=3).

Sample	d(0.1) [µm]	d(0.5) [µm]	<0.2 µm [%]	<1 µm [%]
P CTZRaw	12.201±0.367	30.206±0.292	0.00±0.00	3.3±0.23
T CTZRaw	11.026±0.718	28.847±1.129	0.00±0.00	3.8±0.15
P CTZ2	0.216±0.029	17.181±2.448	5.7±0.34	18.1±1.85
T CTZ2	0.150±0.017	8.564±1.578	27.3±4.56	34.8±3.43

Figures

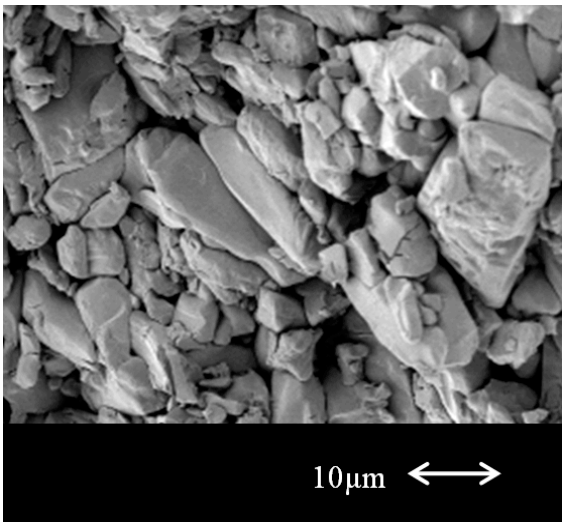

CTZRaw

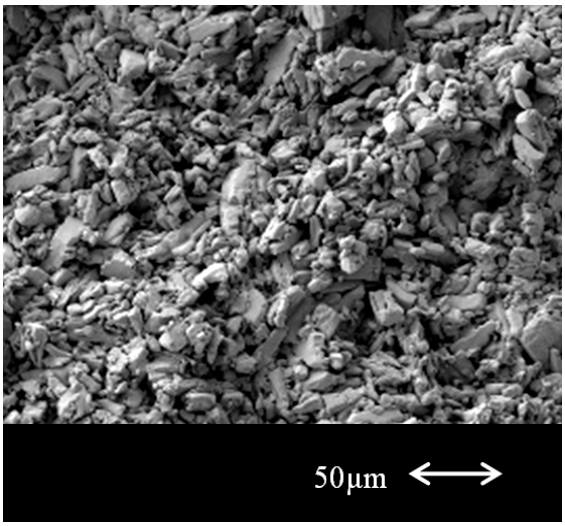

CTZRaw-T

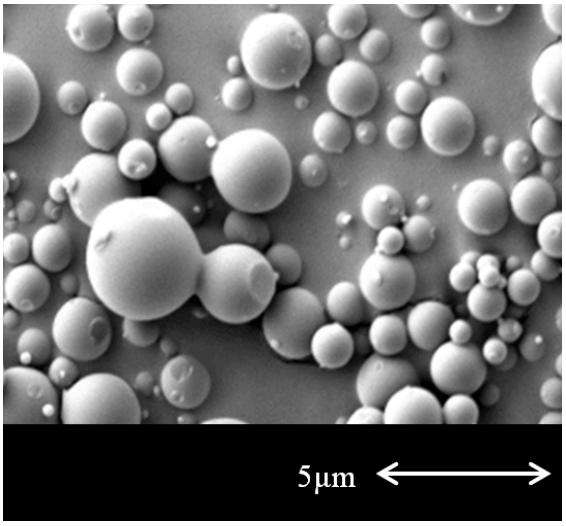

CTZ5

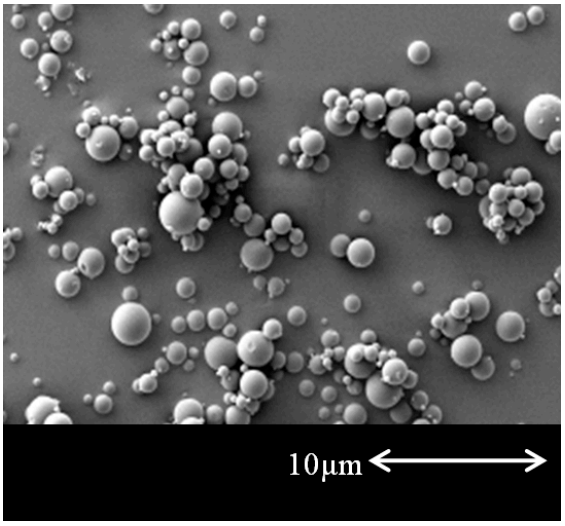

CTZ5

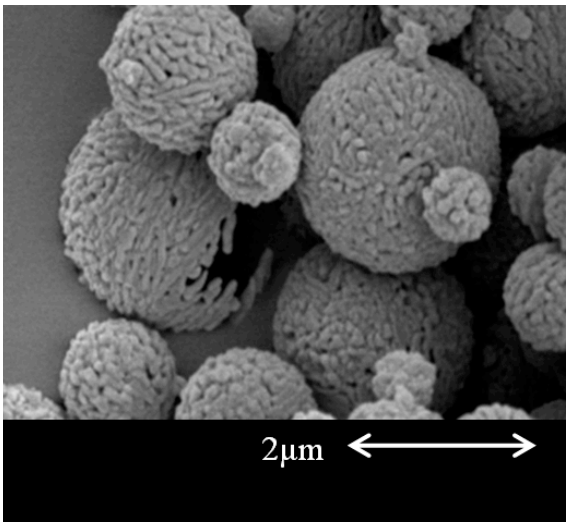

CTZ0.5

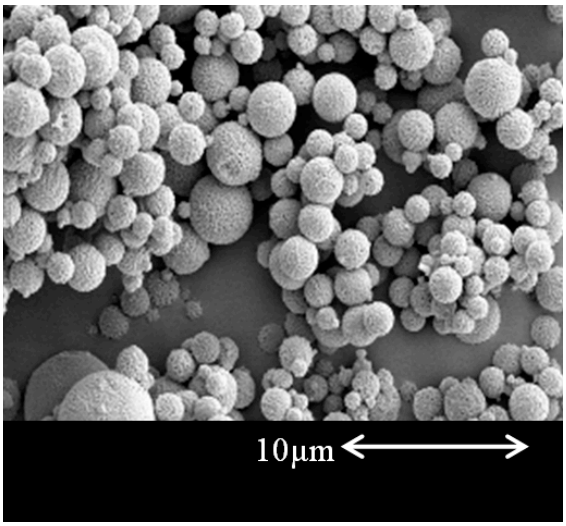

CTZ0.5

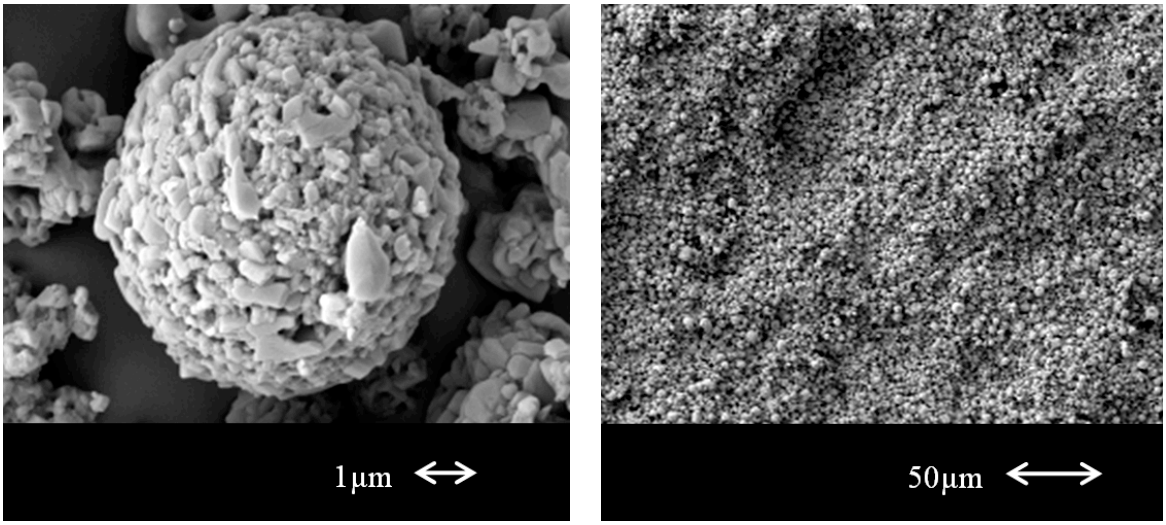

CTZ2 CTZ2-T

Fig. 1. SEM images of: CTZRaw powder, CTZRaw-T (the cross section of the tablet compressed of CTZRaw at 6 kN), CTZ5 powder, CTZ0.5 powder, CTZ2 powder and CTZ2-T (the cross section of the tablet compressed of CTZ2 at 6kN).

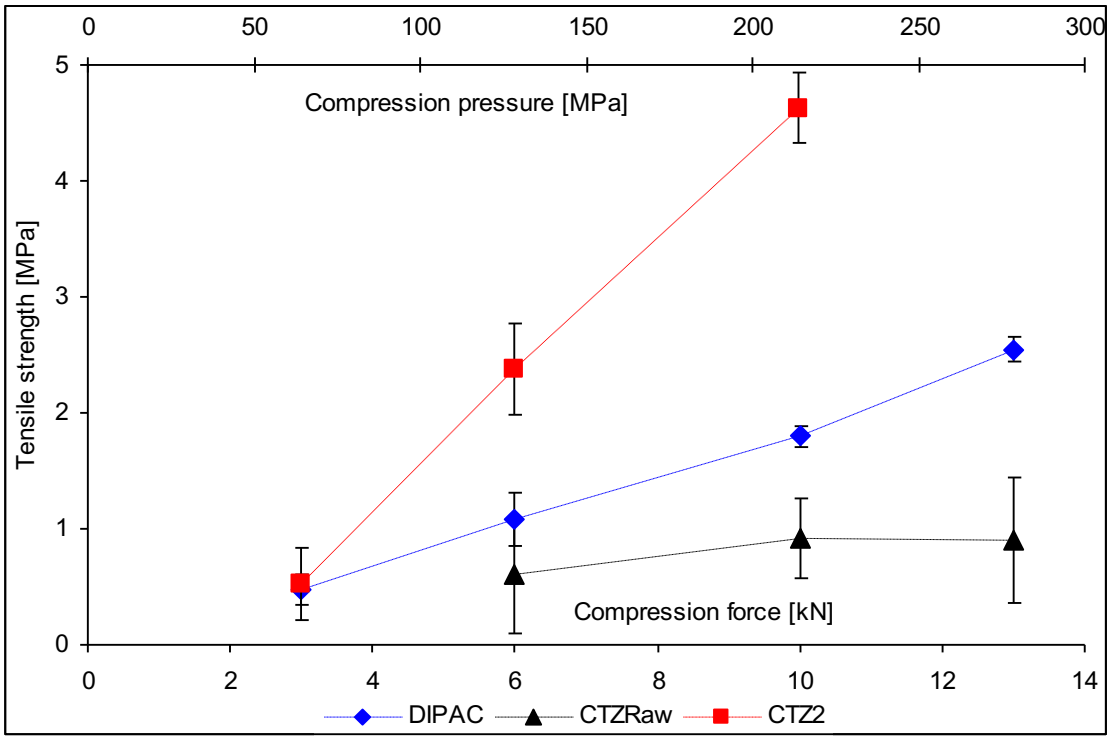

Fig. 2. Tensile strength (σ_t) versus compression force (F) for Dipac^{TM}, CTZRaw and CTZ2. Error bars express relative standard deviation (σ_r) for comparison purposes.

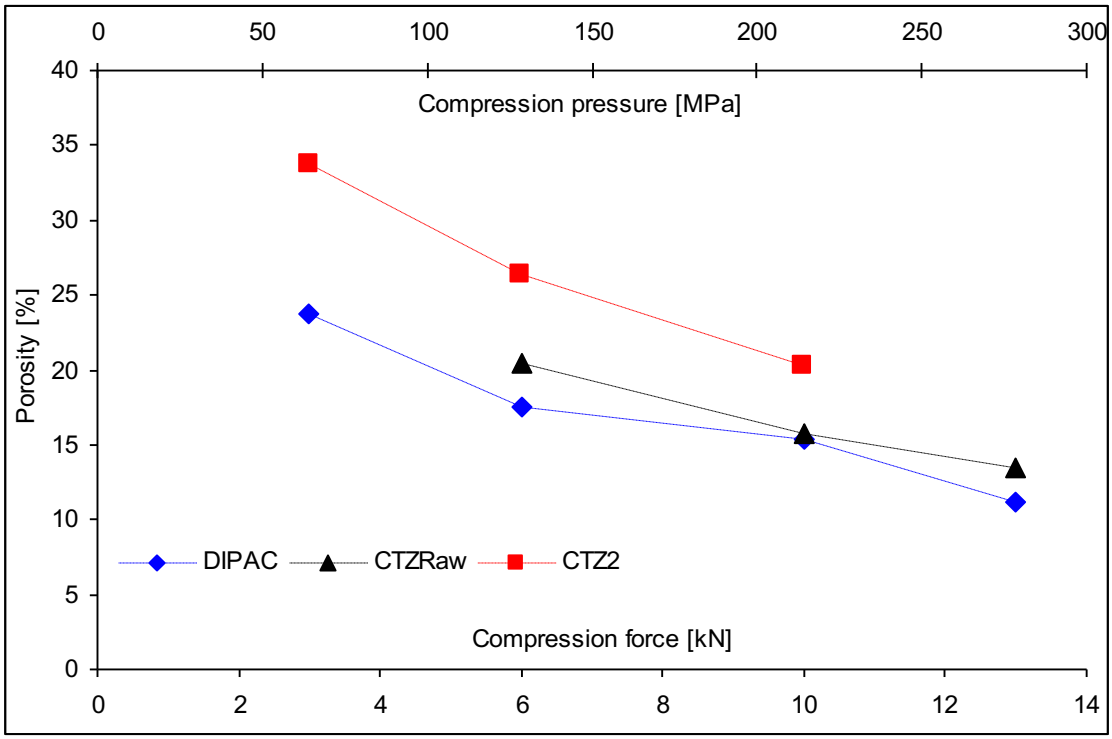

Fig. 3. Porosity of the tablet (ε_t) in relation to compression force (F) for Dipac^{TM}, CTZRaw and CTZ2.

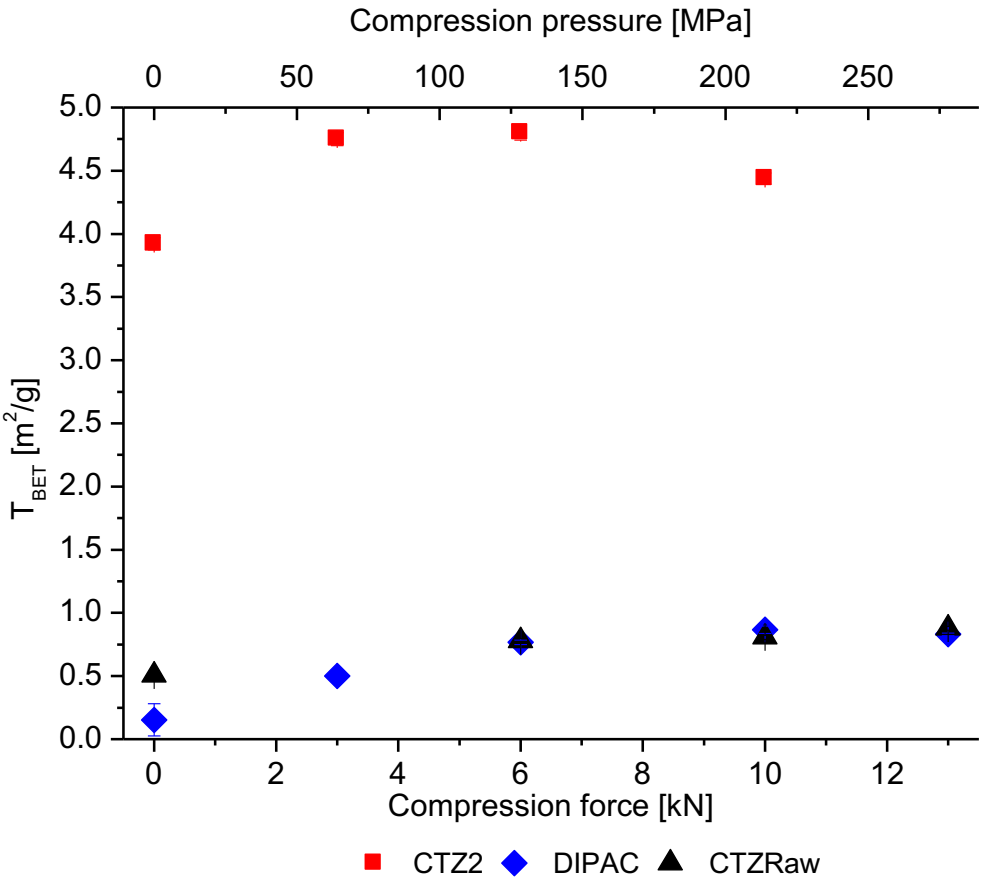

Fig. 4. Specific surface area of the tablet (T_{BET}) in relation to compression force (F) for: Dipac^{TM}, chlorothiazide raw material (CTZRaw) and CTZ nanocrystalline microparticles (CTZ2).

Appendix A

Table A1. Compilation of tablet parameters: force to tensile failure (P), tensile strength (σt), tablet porosity (ε_t) and T_{BET} against compression force (F). σ_r- relative standard deviation.

Formulation	F [kN]	P [N](σ_r)	σt [MPa](σ_r)	ε_t [%](σ_r)	T_{BET} [m^2/g]
CTZRaw	6	24.10(19.80)	0.60(0.49)	20.50(0.31)	0.78±0.02
	10	34.20(12.99)	0.92(0.35)	15.75(0.12)	0.81±0.02
	13	32.56(19.43)	0.90(0.54)	13.50(0.09)	0.88±0.01
CTZ2	3	26.50(23.85)	0.53(0.31)	33.74(0.41)	4.75±0.05
	6	108.30(30.71)	2.38(0.39)	26.45(0.37)	4.80±0.06
	10	190.40(37.58)	4.63(0.31)	20.26(0.33)	4.44±0.04
Dipac™	3	23.70(6.62)	0.47(0.13)	23.80(0.11)	0.50±0.03
	6	49.50(10.27)	1.08(0.22)	17.53(0.21)	0.77±0.02
	10	80.00(3.95)	1.80(0.09)	15.42(0.17)	0.87±0.03
	13	105.80(4.34)	2.55(0.10)	11.14(0.43)	0.83±0.01

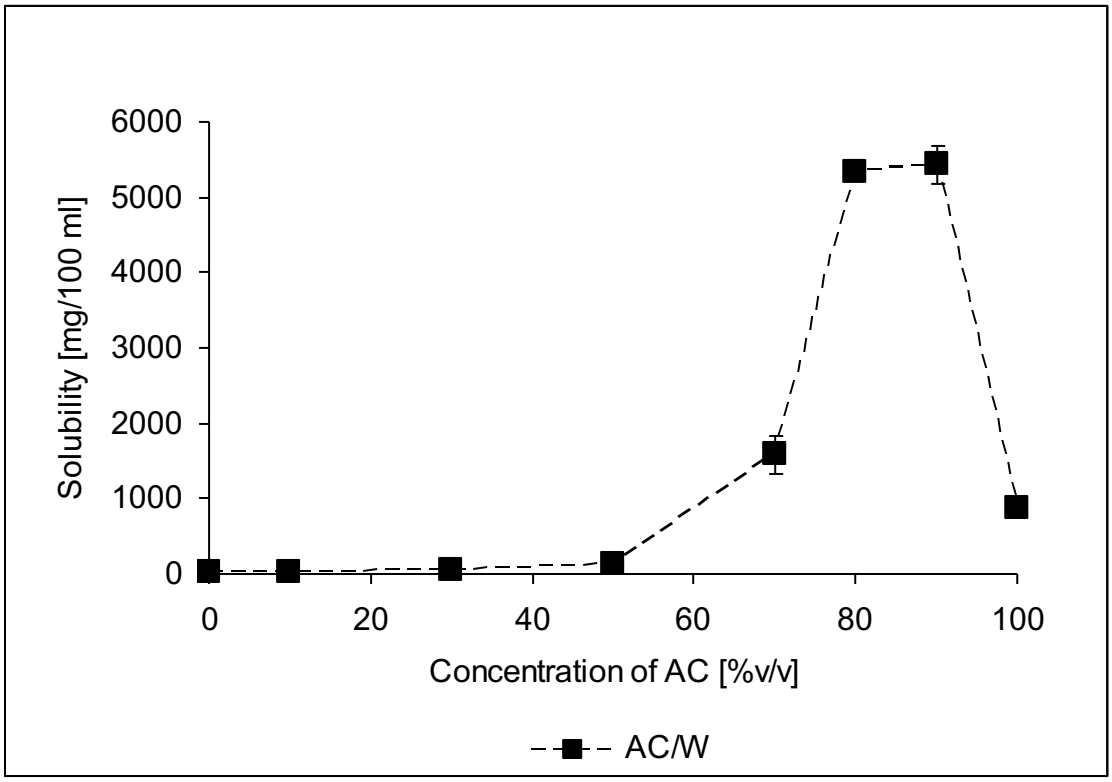

Fig. A1. Solubility of CTZ in acetone, water and acetone/water mixtures.

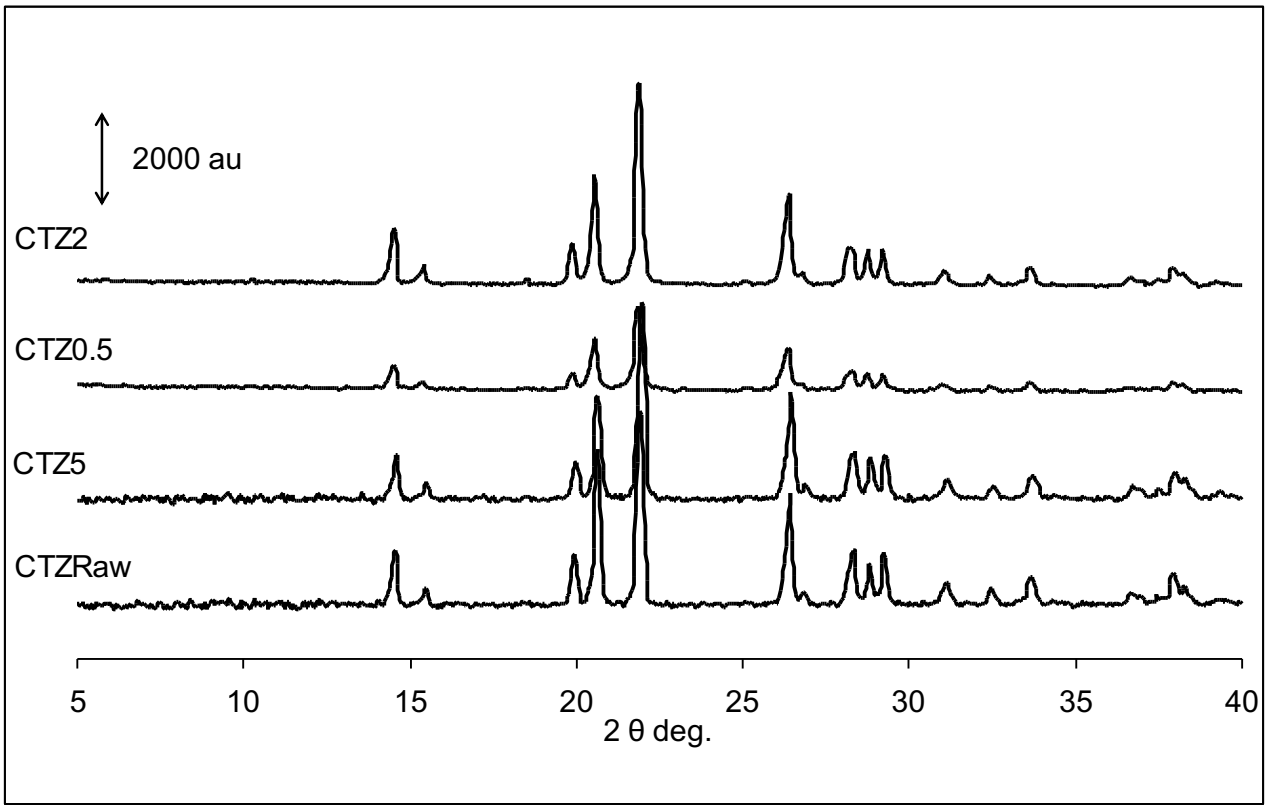

Fig. A2. PXRD of CTZ samples. Abbreviations as per table 1.

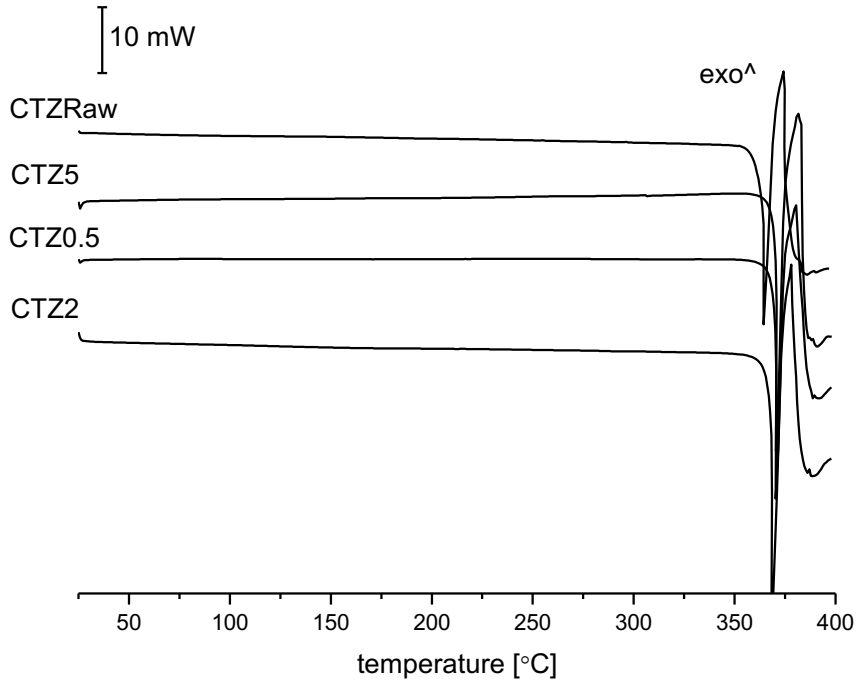

Fig. A3. DSC of CTZ samples. Abbreviations as per table 1.

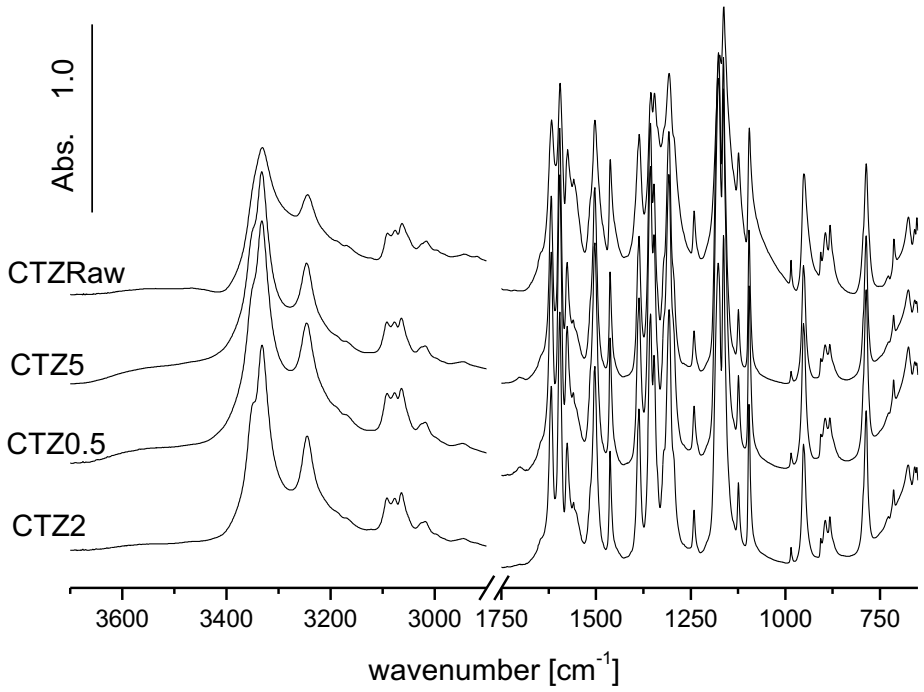

Fig. A4. FTIR of: CTZRaw, CTZ5, CTZ0.5, CTZ2.